Note: Planetary Impact Rates from Ecliptic Comets

Harold F. Levison

Space Studies Department

Southwest Research Institute, Boulder, CO 80302

Martin J. Duncan

Department of Physics, Queen's University

Kevin Zahnle

NASA-Ames Research Center

Matt Holman

Harvard-Smithsonian Center for Astrophysics

and

Luke Dones

Space Studies Department, Southwest Research Institute

To appear in *Icarus*

Abstract

We have re-evaluated the impact rates for the planets from ecliptic comets (ECs) using the integrations in Levison & Duncan (1997). We find that the current impact rates on the giant planets are actually about 4 times smaller than LD97's values due to differences in methods of calculating the relevant timescales. The newly calculated impact rates are listed in Table 1. However, if the objects leaving the Kuiper belt were primarily on high inclination orbits, then the impact rates on the giant planets are larger than those in Table 1 by a factor $\lesssim 2$. We discuss the detail dynamics of objects hitting the giant planets in detail, including measurements of the impact velocities. We find that 21% of the objects that hit Jupiter in our simulations were bound to the planet before the impact. The fraction of bound impactors for Saturn is much lower. Jupiter, Saturn, and Uranus have a significant apex-antapex asymmetry for the unbound impactors.

1. Introduction

In Levison & Duncan (1997, hereafter LD97), we performed an extensive set of numerical integrations of objects that had left the Kuiper belt as they evolved into visible comets. Our goal was to understand the ecliptic comet (hereafter EC) population, which includes the Jupiter-family comets (JFCs), the Centaurs, and, to some extent, the 'scattered comet disk' beyond Neptune. Included in the analysis we presented in LD97 was a crude estimate of the impact rates on the planets from ECs. At the time, we were only interested in an order of magnitude estimate. However, since its publication, the results presented in LD97 have been used to estimate the ages of the surfaces of the Galilean satellites (Zahnle et al. 1998) and Triton (Stern & McKinnon 2000), which require a more accurate estimate. Therefore, we present here a more precise and detailed analysis of the impact rates and characteristics of the impacting bodies.

In LD97, we presented numerical orbital integrations of 2200 massless particles under the gravitational influence of the Sun and the four giant planets, as they evolved from Neptune-encountering orbits in the Kuiper belt. A particle's trajectory was integrated for a billion years or until it either struck the Sun or a planet, or was ejected from the solar system. These integrations were extended to 4 billion years in Duncan & Levison (1997, henceforth DL97). The initial orbits for these particles were chosen from a previous set of integrations of objects that were initially in low-eccentricity, low-inclination orbits in the Kuiper belt but evolved onto Neptune-crossing orbits on timescales between 1 and 4 billion years (Duncan et al. 1995). It is important for the statistical analysis below to note that in LD97, we cloned a test particle 9 times (for a total of 10 particles) if its perihelion distance dropped below 2.5 AU by adding a random number between 0 and 10^{-4} AU to the x, y, and z positions of the particles. Since this must be accounted for in our impact rate estimates below, we divide the trajectory of a particle into 2 parts: that representing the trajectory before its perihelion falls below 2.5 AU (*Stage 1*), and that representing its behavior afterward (*Stage 2*) — only $\sim 1/3$ of the particles ever reached this point. For reasons described in LD97, we will only consider 2000 of the test particles in what follows.

In LD97, we used two methods for calculating the impact rates on the planets in our simulations. For the giant planets, we simply counted the number of impacts. We found that the fraction of ECs that impacted the planets were 0.0088, 0.0028, 0.0050, and 0.0045 for Jupiter through Neptune, respectively. (These numbers are only for the 1 billion year integration presented in LD97; see below.) In order to calculate the impact *rates*, we multiplied these fractions by the rate at which new ECs are being made. We obtained this number by dividing our estimate of the total number of ECs (1.2×10^7) by the *median* dynamical lifetime of the population (4.5×10^7 yrs). At the time we were aware that we should have used the average rather than the median. However, it was not clear how to calculate the average because the simulation only went to a billion years and $\sim 5\%$ of the particles survived. Since we were only interested in an order of magnitude estimate, we decided to use the median. We simply did not foresee the need for a more accurate result.

As discussed above, we calculated the impact rates of comets on the giant planets directly from our calculations. However, we had to estimate the impact rates on the terrestrial planets via other means, because they were not included in our integrations. We followed Öpik (1951) (also see Dones et al. 1999). As a function of time in our simulation, we calculated the rate (probability/yr) that a comet will impact a planet as determined by both the comet's and the planet's instantaneous orbital elements. From this we estimated the average fractional impact rate for the population of ECs as a whole. Finally, we multiplied this value by our estimate of the size of the the EC population (1.2×10^7) to calculate the impact rate on each of the terrestrial planets. Unfortunately, we recently discovered an error in our code that calculated the Öpik impact rates. This error was a function of only the planet's semi-major axis in AU, so the numbers presented in LD97 for all the terrestrial planets, except the Earth, were in error. We will re-evaluate these estimates below.

In §2, we present an analysis of the average dynamical lifetime for an ecliptic comet and recalculate the impact rates for the giant planets. We also evaluate the giant planet impact rates using Öpik's equations. In addition to re-evaluating the impact rates, in §3, we present the detailed dynamics of the impacting bodies. In §4, we discuss methods for scaling our impact rates, which are based on cometary absolute magnitudes, to ones based on cometary radii. We conclude in §5.

2. Impact Rates

Following LD97, we first calculate the impact rates on the giant planets from actual counts of the observed impacts during the simulation. The values that are required to estimate the impact rate on a giant planet are: *i*) the probability that an individual EC will hit a planet (p_X, where X refers to one of the giant planets), *ii*) the total number of ECs in the solar system (N_{EC}), and *iii*) the mean dynamical lifetime of the ECs (L_{EC}).

Before we discuss these parameters, we review the assumptions that we made in LD97 in order to calculate them. We carry these assumptions to the current set of calculations. We assume that the influx rate, R_{KB} from the Kuiper belt has been constant for the age of the solar system. This assumption is clearly not correct since the Kuiper belt must have been more massive in the past (Duncan et al. 1995; Stern 1995; see Malhotra et al. 2000). Unfortunately, we are forced into this assumption because we do not understand how the influx rate varied over the history of the solar system. Fortunately, however, since the vast majority of comets currently in the EC population have only been members for a short amount of time compared to the age of the solar system, this assumption is reasonable if we are only interested in calculating the *current* impact rate on the planets. It should be noted, however, that the impact rates on the planets were most likely significantly higher in the distant past. We also assume that the trajectories of our 2000 test particles are a fair representation of the trajectories of real ECs and that the likely behavior of an EC is not time-dependent (i.e. that a comet leaving the Kuiper belt now will statistically behave the same as comets that left the Kuiper belt billions of years ago.)

There are also two inherent inaccuracies and uncertainties with the analysis presented in LD97, which continue here – both have to do with the total number of ecliptic comets. First, the total number of ECs, N_{EC}, is scaled to the number of observed Jupiter-family comets with absolute magnitudes, H_T, brighter then 9. Since there is no unique relationship between a comet's radius and its absolute magnitude, the range of sizes to which N_{EC} refers to is not clear. Second, the ratio of extinct to active comets is not well known. In LD97, we estimated this ratio to be 3.5, and we adopt this value here. However, it should be noted that our data are consistent with values between 2 and 7. We will return to these issues in §4.

The procedures that we used in LD97 to calculate the p's and N_{EC} are adequate for our task. However, the integrations in LD97 lasted only for a billion years. We have since extended the integrations to 4 billion years (DL97). Therefore, we have reevaluated these numbers using the procedures in LD97, but with the entire 4 billion year integration. We find that the fraction of ECs that impacted the planets were 0.0092, 0.0028, 0.0050, and 0.0050 for Jupiter through Neptune, respectively. In addition, we find that $N_{EC} = 1.3 \times 10^7$. These values are within 10% of the values given in LD97.

The remaining parameter that needs to be evaluated is the mean dynamical lifetime of the ECs, L_{EC}. As described above, we used the median dynamical lifetimes in LD97, which is not accurate enough for our current needs. However, it is not obvious how the mean lifetime should be calculated, given that 1% of the particles survived the 4 billion year integration. We have developed the following argument to determine the appropriate mean.

Suppose that test particles are encountering Neptune for the first time as a Poisson process with rate R_{EC}. Each of these test particles then spends a certain amount of time in the planetary system before being ejected or having a collision. The times are independent and given by a common distribution, G. That is, the probability of surviving for time less than t is $G(t)$. A test particle that was injected at time s will be out of the system at time t if its lifetime is less than $t-s$. The probably of this is $G(t-s)$. If we let $Y(t)$ represent the number of ecliptic comets *still in* the system at time t, then its expected value (Ross 1985) is:

$$E[Y(t)] = R_{KB}\int_0^t (1-G(t-s))ds = R_{KB}\int_0^t (1-G(y))dy. \qquad (1)$$

$E[Y(t)]$ is simply N_{EC}, as defined above. We also are defining $L_{EC} \equiv N_{EC}/R_{KB}$, so:

$$L_{EC} = \int_0^t (1-G(y))\, dy.$$

$G(t)$ can be estimated from the integrations. We see that

$$G(t) \approx 1 - \frac{N(t)}{N(0)},$$

where $N(t)$ is the number of test particles remaining at time t and $N(0)$ is the initial number of test particles. Thus,

$$L_{EC} \approx \int_0^t \frac{N(s)}{N(0)} ds.$$

Since $N(t)$ is basically a "staircase" function that drops by one each time a particle is removed, then

$$L_{EC} \approx \frac{1}{N(0)} \sum_{i=1}^{N(0)} t_i, \qquad (2)$$

where t_i is the minimum of 1) the ejection/collision lifetime of particle i or 2) the age of the solar system.

A time dependent influx rate can easily be incorporated into this argument by replacing Eq.(1) by

$$E[Y(t)] = \int_0^t R_{KB}(s)(1-G(t-s))ds. \qquad (3)$$

As described above, we do not know enough about the history of the solar system to estimate $R_{KB}(s)$. Thus, we adopt Eq.(2) for the remainder of this discussion.

From our integrations and Eq.(2) we find that $L_{EC} = 1.9 \times 10^8$ yr, which makes $R = 0.068$ comets/yr. This should be compared to a value of $R = 0.27$ comets/yr derived in LD97. Thus, the impact rates we calculate here will be ~ 4 times lower than those in LD97.

The first four columns in Table 1 show the detailed numbers used to calculate the impact rates with the above technique. Columns 2 and 3 give the actual number of test particles that hit the planets in our simulations during Stage 1 and Stage 2, respectively. The fraction that impacts a planet is derived by dividing these numbers by 2000 or 20,000 for Stage 1 and Stage 2, respectively. The 'direct' impact rate is then determined by multiplying these numbers by R.

Öpik's equations can also be used to estimate impact rates on the planets. This method has the advantage that it does not suffer from the small-number statistics of direct counting (note the small numbers of impacts for Uranus and Neptune). However, it suffers from inaccuracies in the assumptions used to derive the equations themselves. In addition, the data to which we can apply this technique are temporally sparse, taken once every 10^4 or 10^3 years for the Stage 1 and Stage 2 integrations, respectively. Thus, it is possible that the Öpik technique could miss short-lived events that could change the overall impact rates. Since, however, the Öpik technique has weaknesses that are different from those of the direct count method, we calculate both in the hope that insight into the uncertainties can be gained by a comparison.

There are two ways to apply the Öpik equations to our simulations. We can estimate the likelihood that one of our test particles will hit a planet by $p_i = \sum_{j=0}^{N_{\Delta t}} p'_{ij} \Delta t / P_{ij}$, where P_{ij} is the orbital period of comet i during timestep j, p'_{ij} is the probability that a comet will impact a planet in the next orbit as determined by the Öpik equations, Δt is the temporal spacing of our data set, and $N_{\Delta t}$ is the number of timesteps saved during our 4 billion year simulation. Here the sum is taken over all time. The fraction of comets that will hit a planet is simply the average p_i. To obtain the impact rate, we multiply this average by R as we did above. This method is comparable to the direct count method above, but we use the Öpik equations to estimate the fraction of objects that impact a planet. The results of this calculation are listed in the column labeled *Öpik I* in the table.

We can also use Öpik's equations to estimate the average impact rate for each of the planets. To accomplish this we calculate $\bar{r} = \frac{1}{N_t}\sum_{i=1}^{N_t}\left[\frac{1}{N_{\Delta t}}\sum_{j=0}^{N_{\Delta t}} p'_{ij}\, P_{ij}\right]$, where N_t is the number of particles (or trajectories). To calculate the impact rates we multiply this average by the total number of ecliptic comets, N_{EC}. Notice that we are not using our estimate of the mean dynamical lifetimes in this calculation (which is included in R) and are letting the Öpik equations determine their own timescale. The results of this calculation are listed in the column labeled *Öpik II* in the table.

Except for Uranus, the variation in our estimates of the impact rates listed in Table 1 is at most 36%. Since this value is small compared to the other errors in the estimates of the ages of satellite surfaces (see Zahnle et al. 1998 and §4 for a more complete discussion), we feel that our values are in agreement. The values derived from the Öpik I method tend to be about 25% larger than those derived from Öpik II. We believe that Öpik II results are more reliable since they do not depend on L_{EC}.

Uranus is another issue. There is over a factor of two difference between the impact rates as determined by the Öpik equations and that of the direct count. Also note that the direct count impact rates for Uranus and Neptune are the same. We find this difficult to believe since the number density of ECs at 30 AU should be significantly larger than at 20 AU (see LD97's Figure 8). In addition, only 10 test particles hit each of Uranus and Neptune during our simulations, so the direct count method could have been affected by small number statistics. Thus, we believe that the Öpik values are more reliable.

An independent estimate of the rate that comets strike Jupiter can be based on the recent study by Nakamura & Kurahashi (1998, hereafter NK98). NK98 integrate the orbits of 187 so-called "Jupiter-Interacting Comets" for 30,000 years into the future and 30,000 years into the past. NK98 deduce impact rates by extrapolating the distribution of close encounter distances down to planetary radii; they do not use Öpik's equations. They find that the average impact rate per comet per year is 5×10^{-11} on Earth and 3.6×10^{-7} on Jupiter. The ratio, 7000, agrees well with the values we list in Table 1, especially considering that NK98's initial orbits have a bias toward near-Earth objects. If we scale the NK98 integrations to comets with $H_T < 9$, we find an impact rate on Jupiter of 4×10^{-4} per year, which is again consistent with our results.

Finally, we discuss one other issue concerning the LD97 integrations. At the time that LD97 was published, we assumed that the inclination distribution of Kuiper belt objects was narrow. Although we did perform two runs in LD97 that started with high inclination orbits, these runs were not included in our analysis of impact rates. We continued this practice in the above analysis, even though it has since been realized that a significant fraction of Kuiper belt objects are on high inclination orbits (see `http://cfa-www.harvard.edu/cfa/ps/lists/TNOs.html`). We decided that since we did not know the inclination distribution of objects leaving the Kuiper belt, it would be better to analyze the high inclination objects separately in order to see if this affects the impact rates. Thus, we performed the same analysis as above on the high inclination runs and found that the impact rates were larger by a factor of approximately two. Therefore, since the Kuiper belt is a mixture of low and high inclinations, the inclusion of high inclination objects would increase our estimates of the impact rates, but by less than a factor of two.

3. Impactor Dynamics

When it comes to estimating the ages of satellite surfaces, two important factors are the impact velocities and any asymmetries in the direction from which the impactors approach the planet. We now address these issues by using the test particles that actually impacted one of the planets in our simulation.

Impact Velocities. Figure 1 shows the cumulative distributions of impact velocities for the four giant planets. In the figure, we are actually plotting the velocity of the impactor at large distances from the planet, v_∞. Thus, these numbers do not include the acceleration the objects experience as they approach the planet. The major differences seen in the figure are due to differences in the orbital velocities of the planets and comets as the heliocentric distances increase. Thus, the largest impact velocities occur on Jupiter and the smallest on Neptune.

Bound Impactors. Note that the distributions shown in Figure 1 do not always go to one as the impact velocity goes to zero. This is because a small fraction of the impactors are bound to the planet when they impact. Indeed, these fractions are 0.21, 0.02, 0.1, and 0 for Jupiter through Neptune, respectively. The fraction of bound impactors for Jupiter is similar to the $15 \pm 2\%$ estimated by Kary and Dones (1996). Except for Jupiter, these values suffer from small-number statistics, and so are very uncertain. The median semi-major axis of the bound impactors on Jupiter, a, is 0.25 AU (520 Jovian radii). A Kolmogorov-Smirnov test (hereafter the K-S test; see Press et al. 1986) shows that the jovicentric inclination of the Jovian impacts is consistent with being isotropic, although there is a tendency for the inclinations to be near zero or 180°. This is most likely due to the Kozai resonance which links a drop in inclination with a decrease in pericenter distance (Kozai 1962).

Planetary Apex-Antapex Asymmetries. As seen from one of the giant planets, the ecliptic comets in their neighborhood constitutes a nearly isotropic swarm. However, there may be a small residual apex-antapex asymmetry for planetary impacts. To measure the amount of apex-antapex asymmetry of the impactors, we use K-S tests and model the distribution of impactors as

$$n(<\beta) = 1 - \left(\frac{1}{2} + \frac{1}{2}\cos(\beta)\right)^{\gamma}, \tag{4}$$

where β is the apex angle and γ is a free parameter. Figure 2 shows the K-S probability as a function of γ for the 4 giant planets. It is not clear how to combine the two stages of integrations in this analysis, so we performed this analysis for both Stage 1 (red) and Stage 2 (blue) independently. In addition, only unbound impactors were used to construct these plots. For Jupiter, the Stage 1 impactors are consistent with isotropic in β, but the Stage 2 impactors have only a 4% chance of being isotropic – the best match is for $\gamma = 1.32$. A plot of the distribution of Stage 2 impactors on Jupiter is shown in Figure 3A. Combining these, we find that ratio of impactors at $\beta = 0$ to those at $\beta = 180°$, R_β, is 1.5 on Jupiter. The relation $R_\beta > 1$ implies that there are more impacts on the apex side of Jupiter. This, in turn, implies that most of the impactors have semi-major axes larger than Jupiter.

The K-S test shows that there is only a 24% chance that the Stage 1 Saturnian impactors are isotropic. While this probability is small, it is not possible to rule out isotropy, even though all four of the Stage 1 Saturnian impactors hit the apex side of Saturn. The Stage 2 Saturnian impactors, the distribution of which is shown in Figure 3B, have a 14% chance of being isotropic with a best fit of $\gamma = 0.69$. The relation $\gamma < 1$ implies that there are more impacts on the antapex side of the planet ($R_\beta = 0.61$), which then implies that most of the impactors have semi-major axes less than Saturn. Recall that the Stage 2 integrations consist of objects that had once had $q < 2.5\,AU$, so it is not surprising that they tend to come from inside Saturn's orbit.

For Uranus, there is also a 14% chance that the impactors are isotropic. Here, the K-S probability is maximized at $\gamma = 1.7$, which implies $R_\beta = 2.2$. The data for Neptune show that its impactors are consistent with being isotropic.

4. Scaling Impact Rates

As described above, the impact rates listed in Table 1 refer to comets with absolute magnitudes, H_T, brighter than 9. In LD97, we assumed that there were 40 ECs with $H_T < 9$ and $q < 2$ AU. In order to relate this to the formation of craters on satellites, it is necessary to scale these values to cometary radii. Unfortunately, this is a non-trivial task, since there is no good correlation between the absolute magnitude of a comet (which is based on a comet's activity) and its size. There are several methods available to us to attempt to estimate this scale factor, but none are very satisfactory.

It is convenient to scale impact rates to the number of $1\,km$ diameter comets striking a planet per year. In order to do this, we have to choose a mass distribution. In Zahnle et al. 1998, we used Shoemaker & Wolfe's (1982) $N(> d) \propto d^{-2}$, where d is the comet's diameter. This is a somewhat shallow distribution compared to the theoretical expectation that stray bodies should follow the mass distribution of a collisional cascade in which strength does not depend upon size, for which $N(> d) \propto d^{-2.5}$, but it is in reasonable agreement with crater counts and other indirect estimates of comet sizes (Donnison 1986; Hughes 1988).

By assuming the $N(> d) \propto d^{-2}$ relationship, we present the following alternatives to relate the impact rates in Table 1 to those of objects with $d > 1\,km$. In what follows, we refer to the number by which we must multiply the impact rates in Table 1 in order to scale them to $d > 1\,km$ as S:

i) A possible calibration is based on an assumed relationship between the absolute magnitude of an active comet and its diameter or mass. The two versions most often quoted predict that a comet with $H_T = 9$ has a diameter of $2\,km$ (following Weissman 1990) or a diameter of $0.8\,km$ (following Bailey et al. 1994). Using the above size distribution, we find that $S = 4.0$ and 0.6, respectively.

ii) Shoemaker & Wolfe (1982) estimated that there were 40 JFCs with $q < 1.7\,AU$ and $d > 2.2\,km$ based on calibration of comet diameters to $B(1,0)$ photographic "nuclear" magnitudes. Using LD97's perihelion distribution and the above size distribution, we find that $S = 8.4$.

iii) Following Kary & Dones (1996), we can use the well-determined diameters of the three largest near-Earth JFCs to estimate S: 28P/Neujmin 1, 10P/Tempel 2, and 49P/Arend-Rigaux. All three have diameters $\geq 10\,km$ and perihelia inside $2\,AU$. The list is probably complete. We adopt $N(q < 2AU, d > 10km) = 3$, so we find that $S = 7.5$.

Averaging the four values of S we find a mean of $S = 5$. Multiplying the average of the three impacts rates for Jupiter from Table I by S, we find that the rate of 1-km diameter impacts on Jupiter is 3×10^{-3}/yr, or one impact every 300 years. Unfortunately, the estimates of S range over an order of magnitude, and the situation is even worse when the uncertainty in the size distribution is taken into account. Fortunately, we believe that the situation is likely to improve in the next few years due to the proliferation of large observing projects intended to search for Near Earth Objects (NEOs). These surveys have found several asteroid-like objects in orbits similar to JFCs, which are presumably extinct comets.

Currently, no individual survey has found enough objects with accurate orbits to use the results of these surveys to scale our simulations. However, the rate of sky coverage has increased dramatically in the last year or two because of a new survey known as LINEAR (see `http://www.ll.mit.edu/LINEAR/`), which has only been operating at full capacity since March, 1998. LINEAR is currently responsible for $\sim 70\%$ of all the newly discovered NEOs (G. Williams, personal communication) and its sky coverage will increase since the team has recently obtained a second telescope. We believe that we will have access to a well-understood sample of extinct JFCs within the next year or two that will allows us to constrain our scale factor to within perhaps a factor of 2.

5. Conclusions

We have reevaluated the impact rates for the planets from ecliptic comets (ECs) using the integrations in LD97. We used 3 different methods for the giant planets. The variation for each planet should be viewed as a measure of the uncertainties in these numbers. The main results of these calculations are given in Table 1; we recommend using the last column (Öpik II) as the standard impact rate. The impact rates for the giant planets are factors of 3–8 times smaller than the numbers listed in LD97's Table I, due to differences in calculating the timescales. Analysis of LD97's high inclination runs show that the impact rates on the giant planets could be as much as a factor of two larger than the values in Table 1 if the objects leaving the Kuiper belt were primarily on high inclination orbits.

We have also recalculated impact rates for the terrestrial planets. The new rates are higher for Mercury and Venus, and lower for Mars, than the rates tabulated in LD97. The rates for the Earth are the same.

The impact rates were calculated assuming that the rate at which comets evolve from the Kuiper belt to the EC population has been constant. This assumption is clearly not correct, although we believe that it does not have a large effect on our estimates of the current impact rates. However, most likely these impact rates were significantly higher in the past. Any attempt to use our impact rates to estimate the ages of satellites should take this into account.

The impact rates given in Table 1 are calibrated to active Jupiter-family comets with absolute magnitudes, H_T, brighter than 9. A more common and standardized measure of impact rates is to present them scaled to the number of objects with diameters greater than 1 km striking a planet per year. In order to do this, we find that the values presented in Table 1 should be multiplied by a factor of ~ 5, although there are great uncertainties in this number. Estimates of this scale factor should improve in the next year or two as more extinct JFCs are discovered.

Figure 1 shows the measured velocities for the unbound impactors at each giant planet. However, in Jupiter's case 21% of the impactors were bound to Jupiter before they impacted. The fraction for Saturn is much lower. For all the giant planets besides

Neptune, there was a significant apex-antapex asymmetry for the unbound impactors.

We are grateful for funding from NASA's *Planetary Geology & Geophysics* (HL & LD), *Origins of Solar Systems* (HL), *Planetary Atmospheres* (KZ), *Jovian System Data Analysis Program* (HL), and *Exobiology* programs (HL & KZ). MD is grateful for the continuing financial support of the Natural Science and Engineering Research Council of Canada.

Table 1

Impact Rates of Ecliptic Comets with $H_T < 9$ on the Planets

Planet	Number of Impacts Stage 1	Number of Impacts Stage 2	Rate Direct (comets/yr)	Rate Öpik I (comets/yr)	Rate Öpik II (comets/yr)
Jupiter	7	114	6.3×10^{-4}	5.0×10^{-4}	6.5×10^{-4}
Saturn	4	17	1.9×10^{-4}	2.0×10^{-4}	2.7×10^{-4}
Uranus	10	0	3.4×10^{-4}	1.2×10^{-4}	1.6×10^{-4}
Neptune	10	0	3.4×10^{-4}	2.6×10^{-4}	3.5×10^{-4}
Mercury	–	–	–	4.8×10^{-9}	6.1×10^{-9}
Venus	–	–	–	4.2×10^{-8}	5.4×10^{-8}
Earth	–	–	–	6.2×10^{-8}	8.0×10^{-8}
Mars	–	–	–	1.4×10^{-8}	1.8×10^{-8}

REFERENCES

Bailey, M., Clube, S.V.M., Hahn, G., Napier, W.M. & Valsecchi, G.B. 1994. Hazards due to giant comets: climate and short-term catastrophism. In *Hazards Due to Comets and Asteroids* (T. Gehrels, Ed.), pp. 479–533. Univ. of Arizona Press, Tucson.

Dones, L., Levison, H., & Duncan, M. (1996). On the dynamical lifetimes of planet-crossing objects. In *Completing the Inventory of the Solar System* (T.W. Rettig and J. Hahn, Eds.), pp. 233–244. Astronomical Society of the Pacific Conference Series, Volume 107, San Francisco.

Dones, L., Gladman, B., Melosh, H.J., Tonks, W.B., Levison, H., & Duncan, M. 1999. Dynamical lifetimes and final fates of small bodies: Orbit integrations vs. Öpik calculations. *Icarus*, in press.

Donnison, J.R. 1986. The distribution of cometary magnitudes. *Astron. Astrophys.* **167**, 359–363.

Duncan, M., & Levison, H. 1997. A scattered comet disk and the origin of Jupiter family comets. *Science* **276**, 1670–1672.

Duncan, M., Levison, H., & Budd M. 1995. The dynamical structure of the Kuiper belt. *Astron. J.*, **110**, 3073–3081.

Hughes, D.W. 1988. Cometary magnitude distribution and the ratio between the numbers of long- and short-period comets. *Icarus* **73**, 149–162.

Kary, D.M., & Dones, L. 1996. Capture statistics of short-period comets: Implications for Comet D/Shoemaker-Levy 9. *Icarus* **121**, 207–224.

Kozai, Y. 1962. Secular perturbations of asteroids with high inclination and eccentricity. *Astron. J.* **67**, 591–598.

Levison, H., & Duncan, M. 1997. From the Kuiper belt to Jupiter-family comets: The spatial distribution of ecliptic comets. *Icarus* **127**, 13–32.

Malhotra, R., Duncan, M., & Levison, H. 2000. Dynamics of the Kuiper belt. To Appear in *Protostars and Planets IV* (V. Mannings, A. Boss, and S. Russell eds.). Univ. of Arizona Press, Tucson.

Nakamura, T. & Kurahashi, H. 1998. Collisional probability of periodic comets with the terrestrial planets - An invalid case of analytic formulation. *Astron. J.* **115**, 848–854.

Öpik, E.J. 1951. Collision probabilities with the planets and the distribution of interplanetary matter. *Proc. R. Ir. Acad.* **54A**, 165–199. 1951.

Press, W.H., Flannery, B.P., Teukolsky, S.A., & Vetterling, W.T. 1986. Numerical Recipes. Cambridge University Press, Cambridge.

Ross, S.M. 1985. Introduction to Probability Models, 3rd edition. Academic Press, NY.

Shoemaker, E.M. & Wolfe, R.A. 1982. Cratering timescales for the galilean satellites. In *Satellites of Jupiter* (D. Morrison, Ed.), pp. 277–339. Univ. of Arizona Press, Tucson.

Stern, S.A. 1995. Collisional timescales in the Kuiper disk and their implications. *Astron. J.* **110**, 856–868.

Stern, S.A. & McKinnon, W.B. 2000. Triton's surface age and impactor flux revisited. *Astron. J.*, in press.

Weissman, P.R. 1990. The cometary impactor flux at the Earth. In *Global Catastrophes in Earth History* (V. L. Sharpton and P. D. Ward, Eds.), pp. 171–180. Geological Soc. of America Special Pap. 247, Boulder.

Zahnle, K., Dones, L., & Levison, H.F. 1998. Cratering rates on the galilean satellites. *Icarus*, **138**, 202–222.

Figure Captions

Figure 1 — The cumulative distribution of v_∞ for impactors onto the four giant planets. v_∞ is the impactor velocity at large distances from the planet, and thus these numbers do not include the acceleration the objects experience as they approach the planet. The distributions do not always go to one as the impact velocity goes to zero because a fraction of the impactors are bound to the planet when they impact.

Figure 2 — The probability that the apex-antapex asymmetry of impactors on each of the giant planets is consistent with the model presented in Eq.(4) as a function of γ and as determined by a Kolmogorov-Smirnov (KS) test. Since it is not possible to combine the two stages of integrations in this analysis, we performed this analysis for both Stage 1 (red) and Stage 2 (blue) independently.

Figure 3 — The cumulative distribution of unbound impacts on a planet as a function of the cosine of the apex angle, β. The thick solid black curves show the distribution resulting from our integrations. The blue curve shows what would be expected for an isotropic distribution ($\gamma = 1$ in Equation 4). The red curve represents the best fit for γ. A) Jupiter, Stage 2. B) Saturn, Stage 2. C) Uranus, Stage 1.

FIGURE 1

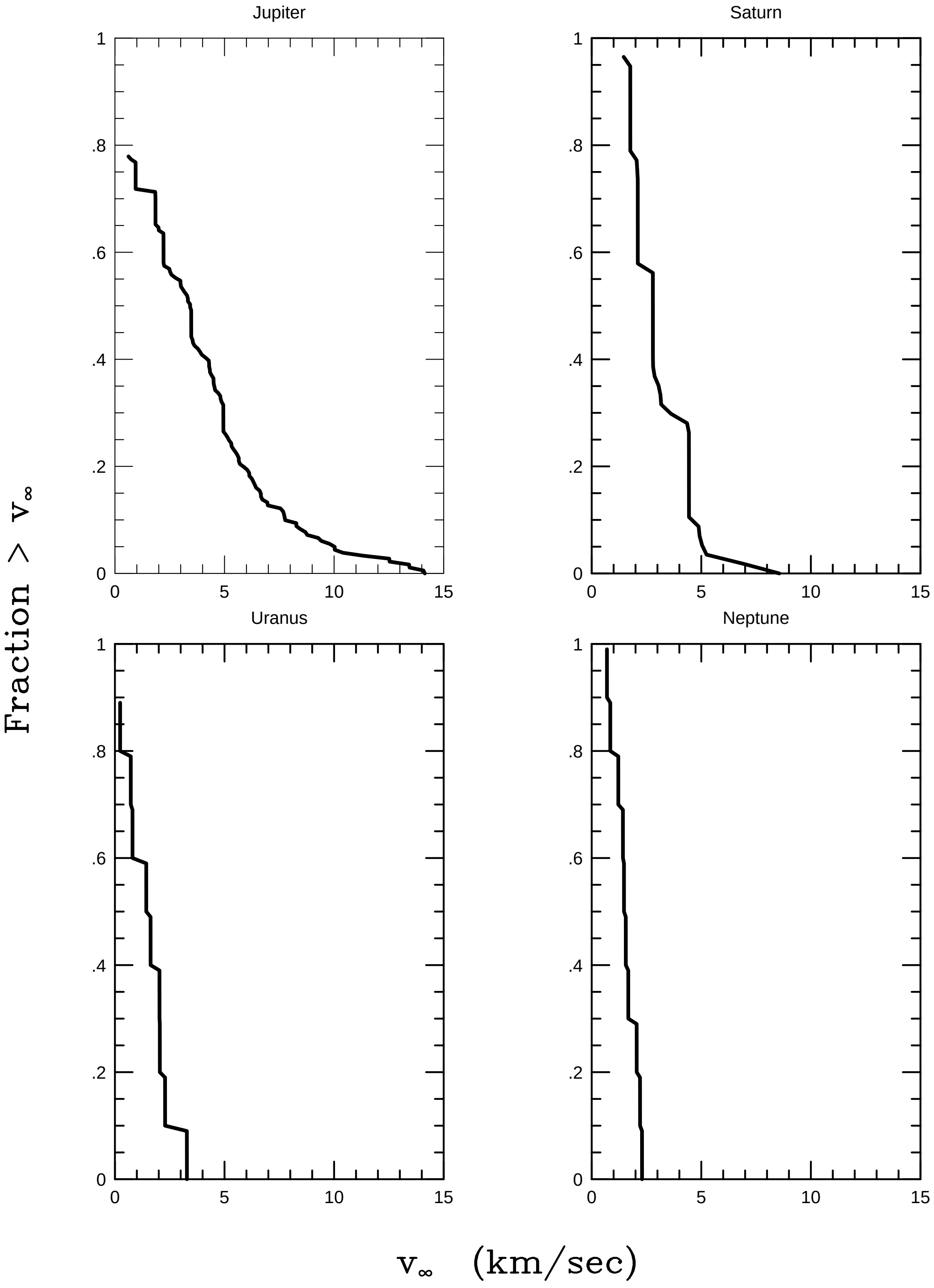

Jupiter
Saturn
Uranus
Neptune
1
.8
.6
.4
.2
0
0
5
10
15
Fraction > v_∞
v_∞ (km/sec)

FIGURE 2

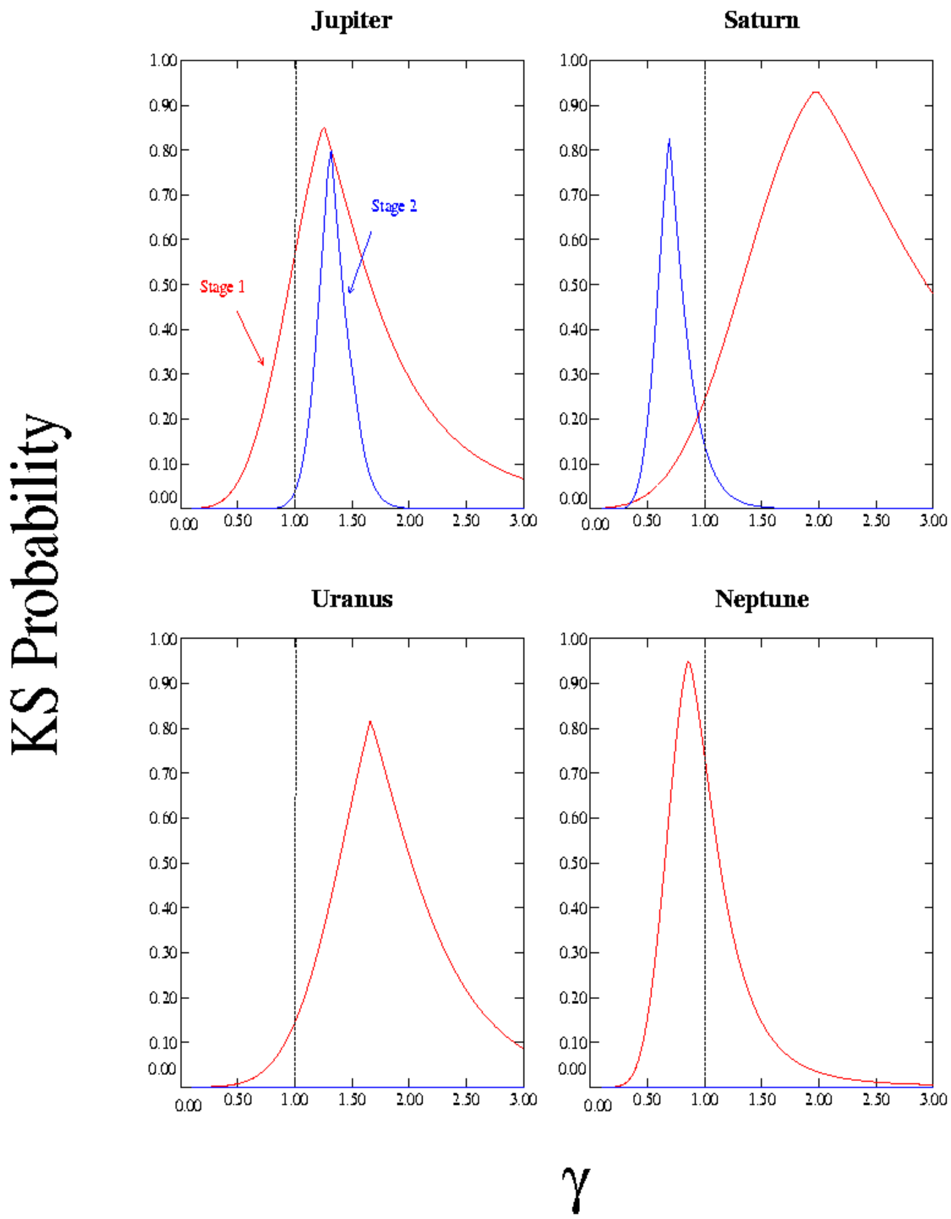

Jupiter
Saturn
Uranus
Neptune
Stage 1
Stage 2
KS Probability
γ

FIGURE 3

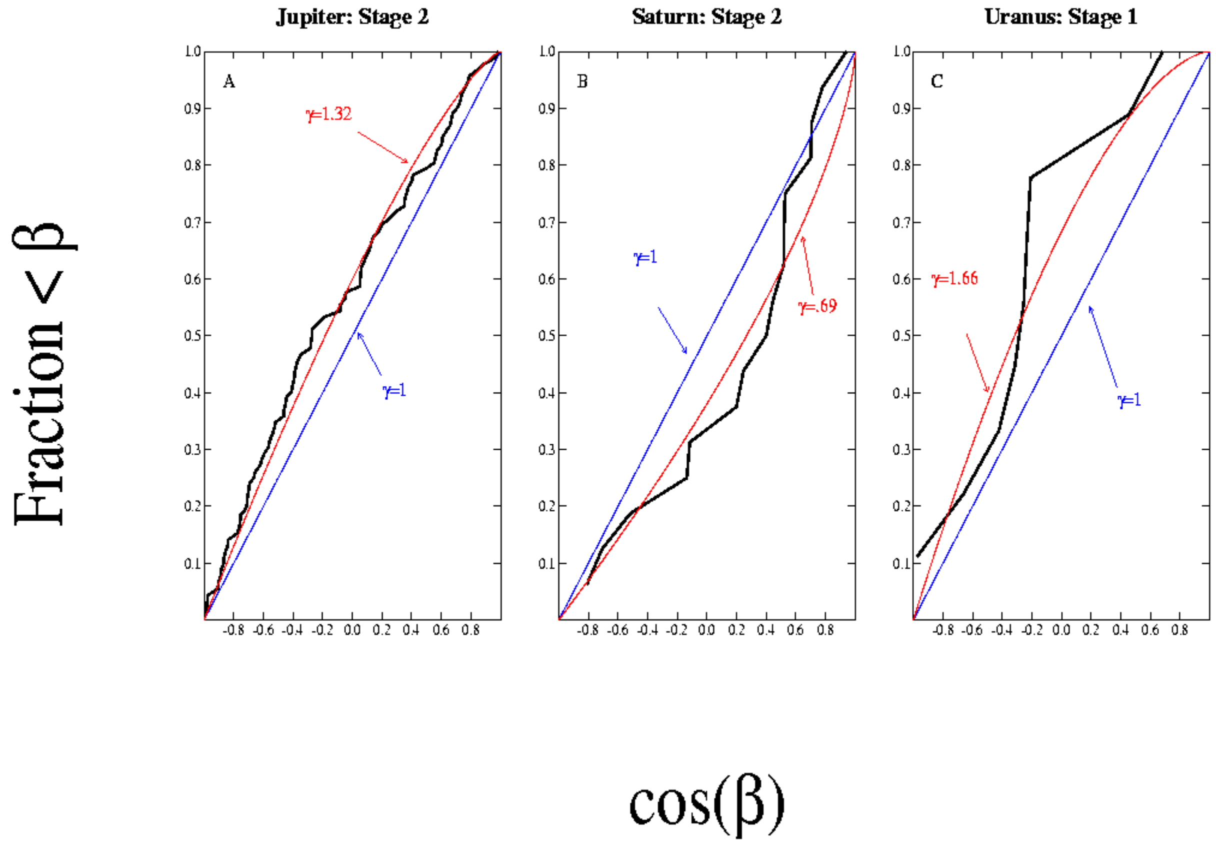

Jupiter: Stage 2
Saturn: Stage 2
Uranus: Stage 1
A
B
C
γ=1.32
γ=1
γ=.69
γ=1.66
Fraction < β
cos(β)